Journal of Solid State Chemistry 181 (2008) 3005–3009

Contents lists available at ScienceDirect

Journal of Solid State Chemistry

journal homepage: www.elsevier.com/locate/jssc

Neutron powder diffraction study of the layer organic–inorganic hybrid iron(II) methylphosphonate-hydrate, $Fe[(CD_3PO_3)(D_2O)]$

Philippe Léone [a,*], Carlo Bellitto [b], Elvira M. Bauer [b], Guido Righini [b], Gilles André [c], Françoise Bourée [c]

[a] Institut des Matériaux Jean Rouxel (IMN), Université de Nantes, CNRS, 2 rue de la Houssinière, BP 32229, FR-44322 Nantes cedex 03, France
[b] CNR, Istituto di Struttura della Materia, via Salaria Km 29.3, CP 10, I-00016 Monterotondo Stazione, Roma, Italy
[c] Laboratoire Léon Brillouin, CEA-CNRS, CEA-Saclay, FR-91191 Gif-s-Yvette cedex, France

ARTICLE INFO

Article history:
Received 4 April 2008
Received in revised form
10 July 2008
Accepted 21 July 2008
Available online 5 August 2008

Keywords:
Iron methylphosphonate
Neutron diffraction
Crystal and magnetic structure

ABSTRACT

The crystal and magnetic structures of the hybrid organic–inorganic layer compound $Fe[(CD_3PO_3)(D_2O)]$ have been studied by neutron powder diffraction as a function of temperature down to 1.5 K. The neutron diffraction pattern recorded at 200 K shows that the fully deuterated compound crystallizes in one of the two known forms of the undeuterated $Fe[(CH_3PO_3)(H_2O)]$. The crystal structure is orthorhombic, space group $Pmn2_1$, with the following unit-cell parameters: $a = 5.7095(1)$ Å, $b = 8.8053(3)$ Å and $c = 4.7987(1)$ Å; $Z = 2$. The crystal structure remains unchanged on cooling from 200 to 1.5 K. Moreover, at low temperature, $Fe[(CD_3PO_3)(D_2O)]$ shows a commensurate magnetic structure ($k = (0,0,0)$). As revealed by bulk susceptibility measurements on $Fe[(CH_3PO_3)(H_2O)]$, the magnetic structure corresponds to a canted antiferromagnet with a critical temperature $T_N = 25$ K. Neutron powder diffraction reveals that below $T_N = 23.5$ K the iron magnetic moments in $Fe[(CD_3PO_3)(D_2O)]$ are antiferromagnetically coupled and oriented along the *b*-axis, perpendicular to the inorganic layers. No ferromagnetic component is observable in the neutron powder diffraction experiment, due to its too small value ($< 0.1\mu_B$).

1. Introduction

Metal phosphonates $M[(RPO_3)(H_2O)]$ (M = divalent metal ion, R = alkyl or aryl group) are typical examples of hybrid layered organic–inorganic compounds [1,2]. They have been intensively studied in the recent past for several reasons, such as ion-exchangers [3], catalysts [4,5], or as hosts in intercalation chemistry [6]. Moreover, they offer the possibility to combine typical properties of organic molecules, like mesomorphism, plastic mechanical properties and optical properties with ones typical of inorganic solids like mechanical strength, long-range magnetic ordering, luminescence, etc. A recent example of the latter is given by ammonium iron(III) carboxyethyl phosphonate [7], which results to be porous and polar. Metal phosphonates of formula $M[(RPO_3)(H_2O)]$ with M = divalent paramagnetic metal ion, are also an interesting class of molecule-based magnetic materials. In particular, at low temperatures the Fe(II) derivatives are "canted antiferromagnets" or "weak ferromagnets" as demonstrated from magnetization measurements [8,9]. The magnetic ordering temperature, T_N, is found to be nearly independent on the interlayer distance, and it ranges between 22 and 25 K [8]. The room temperature crystal structures of several iron(II) phosphonates (methyl [9,10], ethyl [11], propyl [8], butyl [12], octadecyl [8], phenyl [13,14]), have been previously solved either by means of single-crystal or powder X-ray diffraction techniques. These compounds are lamellar, consisting of alternating organic and inorganic layers along one direction of the unit cell. The inorganic layers are made of distorted corner-sharing Fe^{2+} octahedra, surrounded by six oxygen atoms (five from phosphonate groups and one from a water molecule), thus forming a "two-dimensional" lattice; these "inorganic" layers are separated by the organic moieties. $Fe[(CH_3PO_3)(H_2O)]$ add to the mentioned properties of metal phosphonates also another feature: it is polymorphic.

In order to determine the antiferromagnetic structure of the title compound, to check possibly the existence of a crystallographic phase change with temperature, neutron diffraction experiments on powder have been undertaken. Neutron diffraction represents for this purpose the foremost technique. However, studies of organic compounds in general, and of hybrid organic–inorganic metal phosphonates in particular, need the availability of deuterated samples. Up to now only two deuterated manganese(II) phosphonates have been recently studied by neutron powder diffraction [15,16]. With the aim to determine the crystal structure as function of temperature and the magnetic structure of the iron(II) methylphosphonate, we have synthesized

* Corresponding author. Fax: +33 2 40 37 39 95.
E-mail address: Philippe.Leone@cnrs-imn.fr (P. Léone).

0022-4596/$ - see front matter © 2008 Elsevier Inc. All rights reserved.
doi:10.1016/j.jssc.2008.07.032

the fully deuterated compound, Fe[$(CD_3PO_3)(D_2O)$], previously described as the polymorphic form (**2**) [10]. Here we report neutron powder diffraction studies of the fully deuterated compound form (**2**) as a function of temperature down to $T = 1.5$ K.

2. Experimental section

2.1. Synthesis of the ligand $CD_3PO_3H_2$

Per-deuterated methylphosphonic acid was prepared by following the Michelis–Arbuzov method [17,18]. The synthesis of deuterated $CD_3PO_3H_2$ has been carried out by reacting under inert atmosphere CD_3I (7.0 mL, 0.11 mol, Acros 99%) and $(C_2H_5O)_3P$ (17.2 mL, 0.10 mol, Aldrich 98%) in 1:1 ratio under reflux in order to form the corresponding ester [19]. The ester is then hydrolysed with chlorotrimethylsilane and the deuterated acid $CD_3PO_3H_2$ is isolated and characterized by IR spectroscopy.

2.2. Synthesis of Fe[$(CD_3PO_3)(D_2O)$]

Fe[$(CD_3PO_3)(D_2O)$] was prepared according to the method previously described for the synthesis of undeuterated iron(II) compound form (**2**), by using the deuterated methylphosphonic acid ($CD_3PO_3H_2$), deuterated urea, completely dehydrated Fe(II) sulfate and D_2O [9,10]. The compound was characterized by neutron powder diffraction and by IR spectroscopy.

2.3. Physical measurements

The IR spectra were recorded with a Perkin-Elmer FTIR 16F. The neutron diffraction experiments were performed at the Laboratoire Léon Brillouin (CEA-CNRS in Saclay) using the 3T2 and G4.1 diffractometers. Neutron powder diffraction measurements were performed on samples placed in a cylindrical vanadium can and held in a liquid helium cryostat. The high-resolution powder diffractometer 3T2 ($\lambda = 1.2252$ Å) was used for the refinement of the nuclear structure at 30, 120, 160 and 200 K and the high-flux multi-detector (800 cells) G4.1 ($\lambda = 2.4226$ Å) for the determination of the magnetic structure and the thermal evolution of the low-temperature patterns. Ten diagrams were collected between 1.5 and 29.2 K in the 2θ range 13–93°. Rietveld refinement [20] of the nuclear and magnetic structures was performed using the program Fullprof [21] from an initial model based on the crystal structures found previously for Fe[$(CH_3PO_3)(H_2O)$] by X-ray diffraction [10]. The nuclear scattering lengths and iron magnetic form factor were those included in this program.

3. Results and discussion

3.1. Crystal structure

The neutron powder diffraction pattern of Fe[$(CD_3PO_3)(D_2O)$] collected at 200 K, the observed and calculated profiles and the difference between them are shown in Fig. 1. The pattern can be indexed according to the crystal structure of the undeuterated compound [10], orthorhombic symmetry, space group $Pmn2_1$; unit-cell parameters $a = 5.7105(1)$ Å, $b = 8.8072(2)$ Å and $c = 4.7995(1)$ Å; $Z = 2$. Positions for all D atoms have been anisotropically refined; all non-hydrogen atom positions have been refined. Final refined cell parameters, atomic coordinates and isotropic displacement parameters, at 200, 160, 120 and 30 K, are listed in Table 1. The crystal structure of the deuterated sample

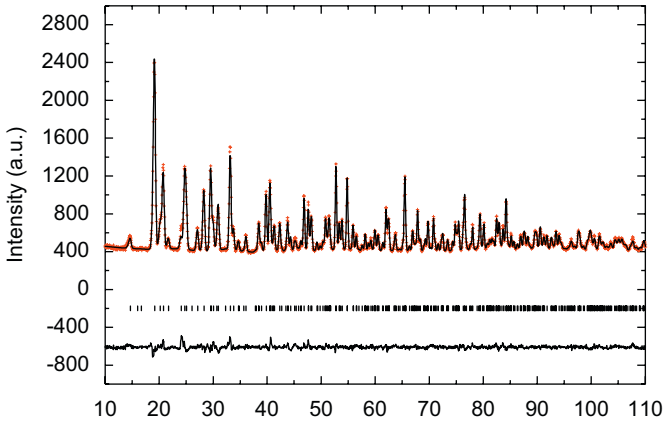

Fig. 1. Observed (cross), calculated (solid line) and difference (solid line at the bottom) neutron diffraction patterns of Fe[$(CD_3PO_3)(D_2O)$] at 200 K (3T2 diffractometer).

was found to be a single phase, corresponding to form (**2**) of Fe[$(CH_3PO_3)(H_2O)$] [9,10]. Figs. 2 and 3 show the layered structure obtained by the Rietveld refinement. The structure is lamellar, consisting of alternating organic and inorganic layers along the *b*-axis of the unit cell. The inorganic layer on the other ends consists of Fe atoms forming a corrugated square two-dimensional array bonded by the O–P–O bridge of the ligand. The CH_3 groups bonded to the phosphorous atom form a bilayer, in which van der Waals interactions are established, being the compound electrically neutral. The crystalline network and space group do not change on cooling from 200 to 30 K and only a small variation of crystal parameters is observed. The crystal structures determined at 200, 160, 120 and 30 K are almost identical.

3.2. Magnetic structure

Magnetization measurements, performed on a powder sample, as function of temperature and field showed that Fe[$(CH_3PO_3)(H_2O)$] is a canted antiferromagnet with a spin canting angle of $\sim 1^\circ$ and a critical temperature T_N of 25 K [9].

Fig. 4 shows neutron diffraction patterns collected on G4.1 diffractometer at two different temperatures well below and well above the critical temperature, i.e. 1.5 and 29.2 K. The pattern recorded at 29.2 K was fitted with cell parameters, atomic coordinates and isotropic displacement parameters, obtained by the refinement of the pattern recorded at 30 K on 3T2 spectrometer. A series of extra peaks is observed at 1.5 K and they are due to the three-dimensional long-range magnetic ordering of the iron magnetic moments. These extra peaks disappear at 23.5 K (see Fig. 5) in agreement with previous magnetization measurements. These magnetic peaks can be indexed in the crystal cell with a wave-vector $k = (0,0,0)$.

Group theory was used in order to determine the magnetic structure and to limit the number of parameters. The calculation of the irreducible representations of the "little" group is based in the subroutine ZAK provided with the program KAREP [22]. The basis vectors, which describe the possible couplings between the components of magnetic moment of the two iron equivalent crystallographic sites, were calculated with Baslreps program included in Fullprof program [21].

The characters table for $Pmn2_1$ group and $k = (0,0,0)$ wave-vector, the decomposition into four irreducible representations for iron site (2a) are given in Table 2, and the basis vectors for these representations in Table 3a. Γ_1 and Γ_3 representations are not compatible with a canted antiferromagnet, because for these

Table 1
Cell parameters (space group $Pmn2_1$), reliability factors, atomic coordinates and isotropic displacement parameters (10^{-3} Å^2) for Fe[$(CD_3PO_3)(D_2O)$] at 200, 160, 120 and 30 K

	x	y	Z	U (U_{eq})
200 K: $a = 5.7105(1)$ Å, $b = 8.8072(2)$ Å, $c = 4.7995(1)$ Å; $R_{Bragg} = 0.054$, $R_f = 0.036$				
Fe(1)	0	0.9736(4)	0.2231*	5(1)
P(1)	0	0.1922(9)	0.6633(11)	10(1)
O(1)	0	0.1717(7)	−0.0258(10)	12(1)
O(2)	0.2153(4)	0.1192(6)	0.5168(7)	12(1)
C(1)	0	0.3880(9)	0.5817(9)	22(1)
D(1A)	0	0.4089(13)	0.3550(12)	*44(5)*
D(1B)	0.1490(8)	0.4448(8)	0.6675(10)	*58(4)*
O(3)	0	0.7892(10)	0.5181(12)	16(1)
D(3)	0.1338(6)	0.7925(8)	0.6465(12)	*45(3)*
160 K: $a = 5.7090(1)$ Å, $b = 8.7943(2)$ Å, $c = 4.7952(1)$ Å; $R_{Bragg} = 0.050$, $R_f = 0.033$				
Fe(1)	0	0.9730(4)	0.2231*	4(1)
P(1)	0	0.1929(8)	0.6620(11)	7(1)
O(1)	0	0.1720(7)	−0.0255(10)	10(1)
O(2)	0.2160(4)	0.1204(5)	0.5169(7)	10(1)
C(1)	0	0.3895(9)	0.5795(8)	19(1)
D(1A)	0	0.4100(11)	0.3532(11)	*36(4)*
D(1B)	0.1493(7)	0.4470(7)	0.6670(9)	*49(3)*
O(3)	0	0.7880(9)	0.5179(11)	10(1)
D(3)	0.1342(5)	0.7947(8)	0.6463(11)	*41(3)*
120 K: $a = 5.7072(1)$ Å, $b = 8.7802(3)$ Å, $c = 4.7929(1)$ Å; $R_{Bragg} = 0.049$, $R_f = 0.029$				
Fe(1)	0	0.9738(5)	0.2231*	1(1)
P(1)	0	0.1913(10)	0.6620(13)	6(1)
O(1)	0	0.1713(8)	−0.0265(12)	9(1)
O(2)	0.2162(5)	0.1204(6)	0.5162(8)	9(1)
C(1)	0	0.3909(10)	0.5794(9)	15(1)
D(1A)	0	0.4138(12)	0.3521(13)	*29(4)*
D(1B)	0.1509(8)	0.4464(8)	0.6662(10)	*41(4)*
O(3)	0	0.7865(10)	0.5174(13)	8(1)
D(3)	0.1340(6)	0.7950(9)	0.6452(13)	*39(3)*
30 K: $a = 5.7051(1)$ Å, $b = 8.7600(3)$ Å, $c = 4.7869(1)$ Å; $R_{Bragg} = 0.050$, $R_f = 0.029$				
Fe(1)	0	0.9742(5)	0.2231*	1(1)
P(1)	0	0.1933(10)	0.6635(13)	2(1)
O(1)	0	0.1719(8)	−0.0267(12)	6(1)
O(2)	0.2152(5)	0.1208(7)	0.5132(9)	6(1)
C(1)	0	0.3940(9)	0.5780(9)	8(1)
D(1A)	0	0.4116(12)	0.3498(12)	*21(4)*
D(1B)	0.1538(6)	0.4474(8)	0.6662(9)	*27(3)*
O(3)	0	0.7873(11)	0.5174(13)	5(1)
D(3)	0.1337(6)	0.7943(9)	0.6431(12)	*29(3)*

* Held invariant in order to define the origin.

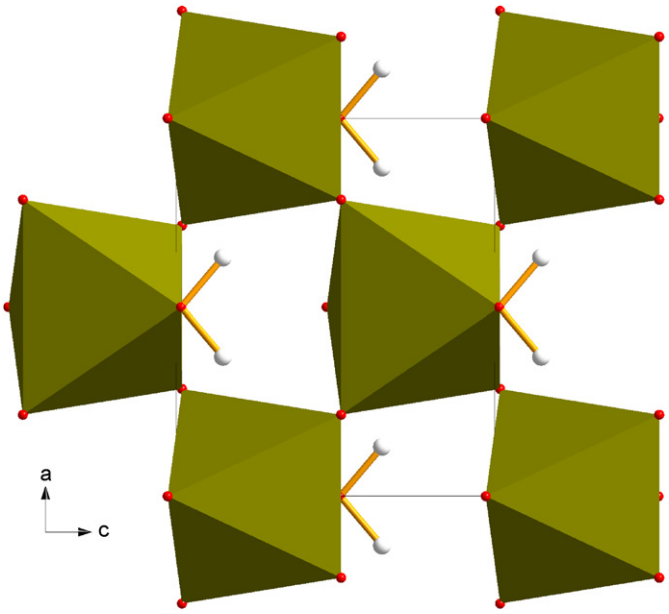

Fig. 2. Inorganic layer made of corner-sharing [$FeO_5(D_2O)$] octahedra.

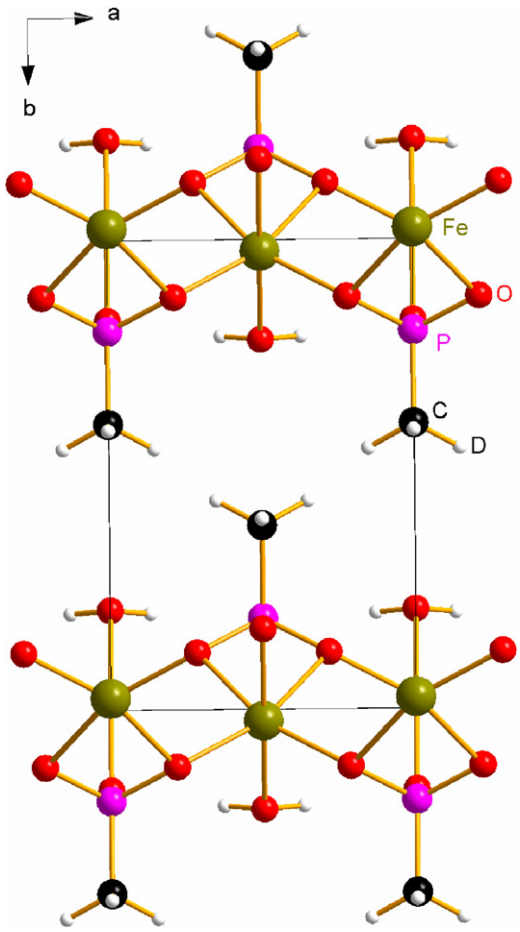

Fig. 3. The crystal structure of Fe[$(CD_3PO_3)(D_2O)$] viewed along the *c*-axis.

representations, the moment vector is defined by only one parameter (M_x). The best refinement is observed for Γ_2 representation. The magnetic reliability factor is 5.7% for the Γ_2 model against 24.5% for the Γ_4 one. Fig. 6 shows observed, calculated and difference neutron diffraction patterns. The results of the refinement are given in Table 3b. The iron magnetic moment reaches $4.26(4)\mu_B$ at 1.5 K. It was not possible to refine the M_z component. Fig. 7 shows the magnetic structure of Fe[$(CD_3PO_3)(D_2O)$]. The iron magnetic moments are oriented perpendicular to inorganic layers. The evolution of the magnetic moment values versus temperature is represented in Fig. 8.

Usually, the Fe^{2+} ion (d^6 high spin) is expected to have a moment of $\sim 4\mu_B$ and the observed value 4.26 is quite high. A possible explanation of this could be the strong preferred orientation, arising from to the lamellar structure: at 29.2 K, in the paramagnetic phase, the Bragg reliability factor is 11.4% without taking account of preferred orientation against 5.9%. Another possible explanation could be the existence of stacking faults: for instance, the (010) peak at $2\theta = 15.9^\circ$ is slightly shifted in position. The M_y antiferromagnetic component, $4.26\mu_B$, and the canting angle of $\sim 1^\circ$ found by magnetic measurements, leads to a M_z ferromagnetic component of $0.075\mu_B$, below the limit value detectable by neutron powder diffraction on G4.1 spectrometer ($0.1\mu_B$).

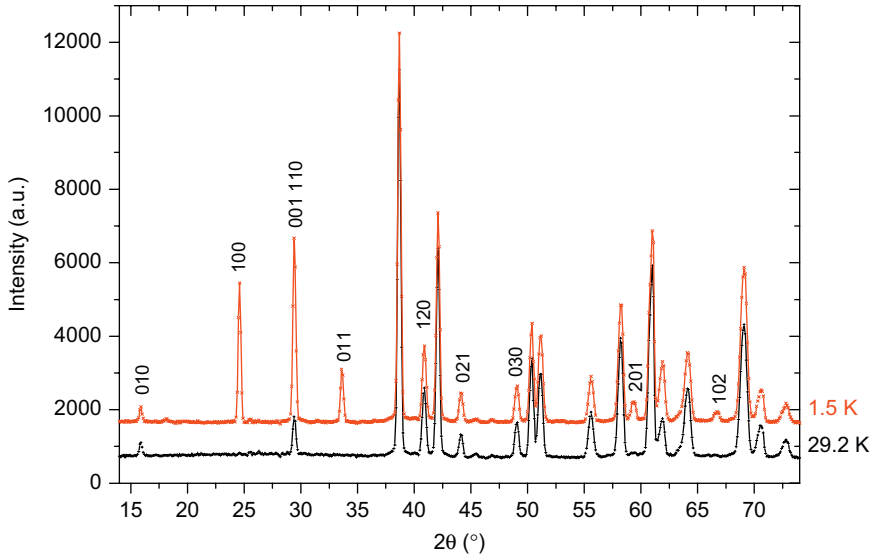

Fig. 4. Part of the neutron powder diffraction patterns of $Fe[(CD_3PO_3)(D_2O)]$ collected at 1.5 and 29.2 K; the diagram at 1.5 K is shifted up.

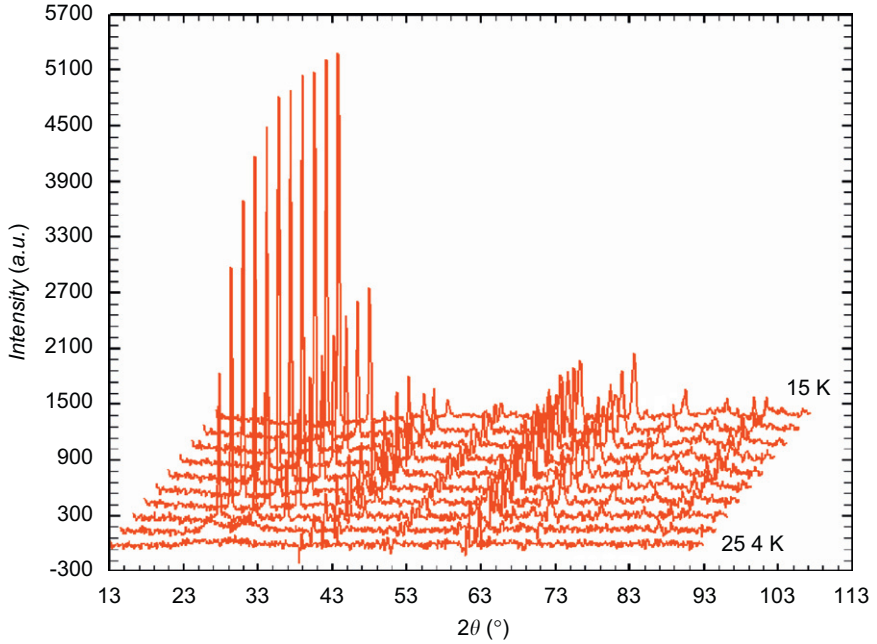

Fig. 5. Difference diffraction diagrams (between considered temperatures and 29.2 K) showing magnetic reflections.

Table 2
Characters table for $Pmn2_1$ group, $k = (0,0,0)$, and decomposition into irreducible representations for the iron site (2a)

	E	2_z	m_x	n_y
Γ	1	1	1	1
Γ_2	1	1	−1	−1
Γ_3	1	−1	1	−1
Γ_4	1	−1	−1	1
Γ	6	0	−2	0
$\Gamma = \Gamma_1+2\Gamma_2+\Gamma_3+2\Gamma_4$				

Table 3a
Basis vectors for the irreducible representations for the iron sites Fe1 and Fe2 (see Table 3b)

	M_x	M_y	M_z
Γ_1	+ −		
Γ_2		+ −	+ +
Γ_3	+ +		
Γ_4		+ +	+ −

4. Concluding remarks

The fully deuterated hybrid organic–inorganic layer compound $Fe[(CD_3PO_3)(D_2O)]$ has been synthesized and studied by neutron powder diffraction as a function of temperature down to 1.5 K. The neutron diffraction pattern recorded at 200 K shows that this compound crystallizes in the orthorhombic symmetry, space group $Pmn2_1$; cell parameters $a = 5.7095(1)$ Å, $b = 8.8053(3)$ Å and $c = 4.7987(1)$ Å; $Z = 2$. It crystallizes in the same space group

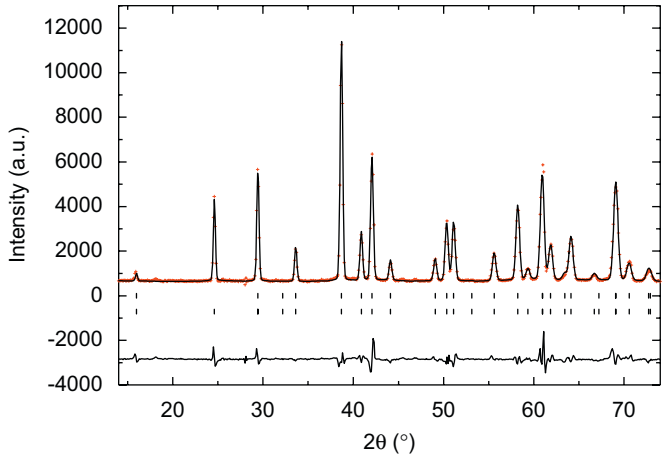

Fig. 6. Observed (cross), calculated (solid line) and difference (solid line at the bottom) neutron diffraction patterns at 1.5 K. The first series of Bragg reflections markers corresponds to the nuclear structure, and the second series to the magnetic structure.

Table 3b
Magnetic moments of iron atoms and refinement reliability factors at $T = 1.5$ K

Atom	x	y	z	M_x	M_y	M_z	M (μ_B)
Fe1	0	0.9742	0.2231	0	4.26 (4)	0	4.26 (4)
Fe2	0.5	0.0258	0.7231	0	−4.26 (4)	0	4.26 (4)
Phase 1	Crystalline structure	$R_{Bragg} = 5.76$	$R_f = 4.76$				
Phase 2	Magnetic structure	$R_{magnetic} = 5.65$					

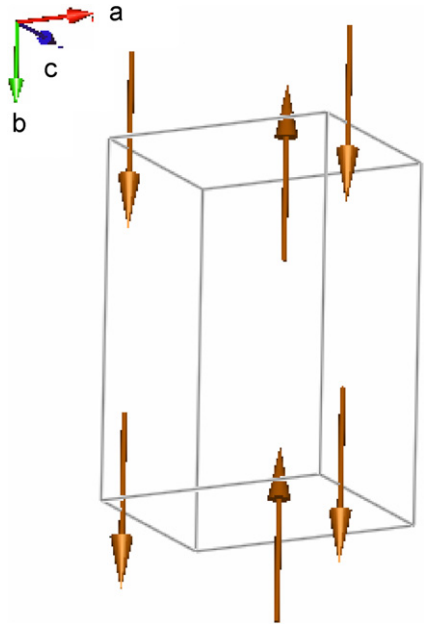

Fig. 7. The magnetic structure of Fe[$(CD_3PO_3)(D_2O)$].

as form (**2**) of the undeuterated Fe[$(CH_3PO_3)(H_2O)$] and the crystal structure remains the same on cooling from 200 to 1.5 K. Below 23.5 K, Fe[$(CD_3PO_3)(D_2O)$] shows a commensurate magnetic structure ($k = (0,0,0)$). This structure is consistent with a canted antiferromagnet with a critical temperature of $T_N = 25$ K, as revealed by bulk susceptibilities performed previously on Fe[$(CH_3PO_3)(H_2O)$]. The iron magnetic moments are antiferromagneticaly coupled and oriented along the *b*-axis,

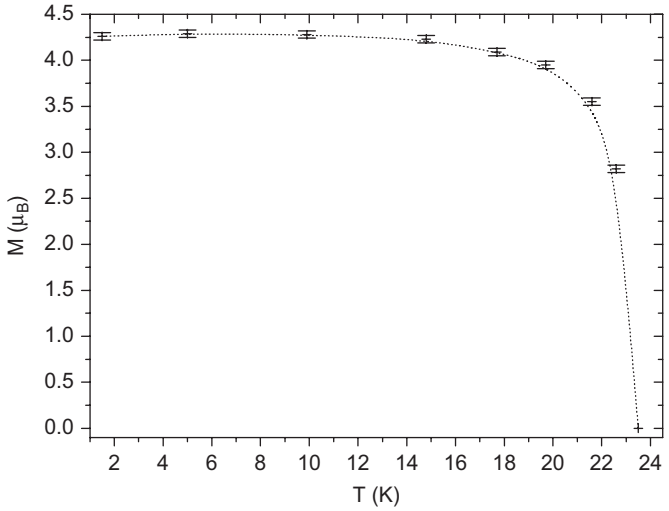

Fig. 8. Evolution of the magnetic moment versus temperature (the curve is just a B-spline interpolation).

perpendicular to the inorganic layers. The spin canting is too small to be detected in the powder neutron diffraction data. Contrary to Mn[$(CD_3PO_3)(D_2O)$] [16], no significant asymmetry is detected in the background of the (100) peak at $2\theta = 24.5^\circ$ and then no short-range ordering is evidenced.

Acknowledgments

This work is supported by Italian MIUR FIRB 2001 Program. Thanks are due to CNR (Italy) and the CNRS (France) for the support in the framework of their bilateral collaboration agreement. One of us (C.B.) likes to thank Dr. Patrizia Imperatori for helpful discussions.

References

[1] G. Alberti, Comprehensive supramolecular chemistry, in: J.M. Lehn (Ed.), Pergamon Press, New York, 1996, vol. 7, pp. 151–185.
[2] A. Clearfield, Progr. Inorg. Chem. 47 (1998) 371–510.
[3] B. Zhang, A. Clearfield, J. Am. Chem. Soc. 119 (1997) 2751–2752.
[4] G. Cao, H. Lee, V.M. Lynch, T.E. Mallouck, Inorg. Chem. 27 (1988) 2781–2785.
[5] G. Cao, H. Lee, V.M. Lynch, L.M. Yacullo, Chem. Mater. 5 (1993) 1000–1006.
[6] K.J. Martin, P.J. Squattrito, A. Clearfield, Inorg. Chim. Acta 155 (1989) 7–9.
[7] A. Anillo, A. Altomare, A.G.G. Moliterni, E.M. Bauer, C. Bellitto, M. Colapietro, G. Portalone, G. Righini, J. Solid State Chem. 178 (2005) 306–313.
[8] C. Bellitto, E.M. Bauer, P. Léone, A. Meerschaut, C. Guillot-Deudon, G. Righini, J. Solid State Chem. 179 (2006) 579–589.
[9] C. Bellitto, F. Federici, M. Colapietro, G. Portalone, D. Caschera, Inorg. Chem. 41 (2002) 709–714.
[10] P. Léone, P. Palvadeau, K. Boubekeur, A. Meerschaut, C. Bellitto, E.M. Bauer, G. Righini, P. Fabritchnyi, J. Solid State Chem. 178 (2005) 1125–1132.
[11] B. Bujoli, O. Pena, P. Palvadeau, J. Le Bideau, C. Payen, J. Rouxel, Chem. Mater. 5 (1993) 583–587.
[12] J. Le Bideau, C. Payen, B. Bujoli, P. Palvadeau, J. Rouxel, J. Magn. Magn. Mater. 140 (1995) 1719–1720.
[13] A. Altomare, C. Bellitto, S.A. Ibrahim, M.R. Mahmoud, R. Rizzi, J. Chem. Soc. Dalton (2000) 3913–3919.
[14] C. Bellitto, F. Federici, A. Altomare, S.A. Ibrahim, R. Rizzi, Inorg. Chem. 39 (2000) 1803–1808.
[15] S. Carling, G.E. Fanucci, D.R. Talham, D. Visser, P. Day, Solid State Sci. 8 (2006) 321–325.
[16] S. Carling, D. Visser, P. Day, J. Mater. Chem. 16 (2006) 2698–2701.
[17] A. Michaelis, R. Kaehne, Chem. Ber. 31 (1898) 1048.
[18] A.E. Arbuzov, J. Russ. Phys. Chem. Soc. 38 (1906) 687.
[19] V.J. Carter, J.P. Kujanp, F.G. Riddell, P.A. Wright, J.F.C. Turner, C.R.A. Catlow, K.S. Knight, Chem. Phys. Lett. 313 (1999) 505–513.
[20] H.M. Rietveld, J. Appl. Crystallogr. 2 (1969) 65.
[21] J. Rodriguez Carvajal, Abstracts of the Satellite Meeting of the XV Congress of the IUCr, Toulouse, 1990, 127pp.
[22] E.R. Hovestreydt, M.I. Arroyo, S. Slatter, H. Wonchatescheck, J. Appl. Crystallogr. 25 (1992) 544.